Catal Lett (2008) 120:204–209
DOI 10.1007/s10562-007-9270-y

Comparative Study of Rubidium and Cesium as Promoters in Carbon-supported Ruthenium Catalysts for Ammonia Synthesis

Yu. V. Larichev · D. A. Shlyapin · P. G. Tsyrul'nikov · V. I. Bukhtiyarov

Received: 3 May 2007 / Accepted: 4 September 2007 / Published online: 18 September 2007

Abstract Sibunit-supported Ru-catalysts promoted with cesium or rubidium compounds have been comparatively studied with XPS. The cesium promoter interacts both with support and with active component. The absence of the promoter–support interaction in the case of rubidium provides a stronger interaction between promoter and active component compared to the cesium-based catalysts. These differences in the promoter–support and promoter–metal interactions are exhibited when a sequence of ruthenium and alkali introduction are changed.

Keywords Ammonia synthesis · Ruthenium catalysts · Cs · Rb · Promoter–support interaction · XPS · TEM

1 Introduction

The catalytic synthesis of ammonia from nitrogen and hydrogen on a promoted iron catalyst (the Haber–Bosch process) is the main industrial method of nitrogen fixation. Severe conditions of this process ($T > 450$ °C and $P = 30$ MPa [1, 2]) motivate the search of new catalysts exhibiting high activity in this reaction at lower temperatures (250–350 °C). This could allow attainment of the required equilibrium yield of ammonia (20%) at lower pressures (3–5 MPa) and, thereby, reduction in power inputs of the process.

Since the 1970s, ruthenium catalysts for ammonia synthesis at moderate conditions (250–400 °C, 3.0–5.0 MPa) have been developed. Carbon-supported ruthenium catalysts modified with alkaline (Cs, Rb, K) and alkaline-earth metal compounds are among the most promising commercial catalysts now [3–5]. Previous study [6] demonstrated that the activity of Ru–Cs^+/C (Sibunit) catalysts strongly depends on the sequence of introduction of ruthenium and promoter (cesium compounds). Indeed, active catalyst is produced when ruthenium is supported on the carbon material (Sibunit) before the introduction of cesium. A reverse order (first, cesium and then ruthenium) leads to inactive samples. Contrary to the Ru–Cs^+/C catalysts, samples, which is used rubidium as promoter (Ru–Rb^+/Sibunit), show only a minor effect of the order of introduction of ruthenium and promoter on the catalysts activity. Elucidation of the reasons for these distinctions in behavior of two systems will promote our understanding the nature of these multicomponent catalysts and, consequently, may help to simplify and cheapen the production of ruthenium catalysts for industrial ammonia synthesis.

In this work we perform a comparative physico-chemical study of the cesium- and rubidium-promoted ruthenium catalysts for ammonia synthesis.

Yu. V. Larichev · V. I. Bukhtiyarov (✉)
Boreskov Institute of Catalysis, Novosibirsk 630090, Russia
e-mail: vib@catalysis.ru

D. A. Shlyapin · P. G. Tsyrul'nikov
Institute of Hydrocarbons Processing, Omsk 644040, Russia

V. I. Bukhtiyarov
Novosibirsk State University, Novosibirsk 630090, Russia

2 Experimental

2.1 Sample Preparation

The graphite-like material Sibunit [7] with a specific surface area of 320 m^2/g was used as a carbon support (C). The samples were prepared by the impregnation of Sibunit

with an aqueous solution of a carbamide complex of ruthenium followed by reduction in a flow of hydrogen at T = 400 °C for 4 h. Then the Ru/C samples were impregnated with an aqueous cesium nitrate or rubidium nitrite solutions and, after drying at 100 °C, calcined in an atmosphere of argon at 300 °C for 2 h. At the final stage, the samples were additionally treated with hydrogen at 300 °C. The promoter-to-ruthenium molar ratio was equal to 2.5. The concentrations of Cs, Rb, and Ru in the samples were equal to 13.6, 8.7, and 4.0 wt.%, respectively. The above described procedure was used also to prepare reference samples, the promoted Sibunit samples (Cs^+/C) and (Rb^+/C) with the same concentrations of cesium and rubidium as those in ruthenium catalysts.

2.2 Catalyst Testing

Activity of the synthesized catalysts was determined.[1] in a double-reactor flow setup at temperatures of 320 and 350 °C, gas mixture (H_2:N_2 = 3:1) pressures of 0.6 and 3.0 MPa, and volume flow rates of (1.2–15.0) × 10^3 h^{-1}. Weight of a sample loaded into the reactor was 1.4 g. The catalyst activity was characterized by the amount of ammonia expressed in mmol which is released in a unit time (1 h) and referred to 1 g Ru under standard conditions.

2.3 Catalyst Characterization

2.3.1 X-ray Photoelectron Spectroscopy (XPS)

XPS spectra were recorded using a VG ESCALAB HP electron spectrometer with AlK_α non-monochromatic radiation ($E_{h\nu}$ = 1486.6 eV). We analyzed both the survey photoelectron spectra and narrow regions from the main catalyst components: ruthenium (Ru3d), carbon (C1s) cesium (Cs3d) or rubidium (Rb3d), as well as from oxygen (O1s). XPS lines of impurities other than oxygen were not detected. Before the measurements, the spectrometer was calibrated against the binding energies of $Au4f_{7/2}$ (84.0 eV) and $Cu2p_{3/2}$ (932.6 eV) core levels. The good conductivity of the Sibunit eliminates the charging effect appeared for dielectric samples as a result of photoelectron emission. Therefore, all core-level binding energies presented in this work were determined from original XPS spectra without any corrections. The samples were pressed into a Ni gauze spot welded to sample holder, placed into the spectrometer preparation chamber, evacuated to 10^{-5} Pa, and then transferred to the analytic chamber, where the spectra were measured. The spectra from one sample were taken twice—before and after additional treatment of the sample in hydrogen which was performed in the preparation chamber at 350 °C and 0.1 MPa for 1 h. The relative surface concentrations of the elements expressed as atomic ratios were calculated from the areas of the corresponding XPS lines (I_x and I_C) corrected for atomic sensitivity factors [8] using the following equation:

$$n_x/n_C = \frac{\frac{I_x}{ASF_x}}{\frac{I_C}{ASF_C}}$$

where $n_{x(C)}$ is the concentration of element x (carbon), ASF_x and ASF_C are the atomic sensitivity factors of the element and carbon, respectively.

2.3.2 High-resolution Transmission Electron Microscopy (HR-TEM)[2]

A JEOL JEM-2010 transmission electron microscope operating at 200 kV was used for measurement of high-resolution TEM images. For the TEM measurements a small quantity of sample powder taken out of the ampoule filled with argon was suspended in hexane. The suspension was deposited on a perforated carbon film fixed on the copper gauze. Evaporation of the solvent was performed before loading the sample into microscope. The linear sizes of 400–600 particles were measured for each sample to obtain size distribution of Ru particles (TEM histogram) and to determine the mean particle size. X-ray microanalysis (EDX) of the element composition of the objects observed in TEM images was performed using an EDX energy-dispersion spectrometer with a Si(Li) detector (resolution of 130 eV).

2.3.3 Chemisorption Measurements[3]

Dispersion of Ru particles was determined by selective chemisorption of CO using an AutoChem II 2920 instrument (Micromeritics). The chemisorption stoichiometry of Ru/CO = 1:1 was taken to calculate the dispersion [9]. The samples were loaded in air and then reduced with hydrogen for 15 min at 200 °C (the flow rate of 25 mL/min), which was followed by a series of CO pulses (10% CO in He) at room temperature to provide total saturation of the surface of supported metal with chemisorbed CO molecules.

[1] The catalytic activity of the samples was tested by Dr. N. M. Dobrynkin.

[2] TEM images were obtained by Dr. V. I. Zaikovskii.

[3] Chemisorption measurements were made by Dr. L. B. Okhlopkova and Prof. A. S. Lisitsyn.

3 Results and Discussion

The data of catalytic activity testing presented in Table 1 shows the activity of the Ru–Cs^+/C catalysts to depend strongly on the sequence of promoter and ruthenium introduction. If promotion of the sample with cesium compounds occurs after impregnation of ruthenium salt followed by its reduction with H_2, the catalyst exhibits a rather high activity in ammonia synthesis. If cesium and ruthenium are introduced in the reverse order (first—the promoter and then ruthenium), activity of the sample is below the sensitivity limit. When rubidium is used as a promoter, a sequence of metal and promoter introduction does not affect so significantly the catalyst activity: drop of activity is not more than 25% (Table 1). Under the studied conditions, the activity of non-promoted sample was below the sensitivity limit.

Figure 1 shows typical TEM micrographs of the Ru–Rb^+/C and Ru–Cs^+/C catalysts which demonstrate contrast images of the spherical Ru particles with different sizes. One can also see that the Ru particles are covered with a thin (<1 nm) layer of disordered structure. The EDX local elemental analysis (Fig. 2) shows that this layer contains compounds of promoter (both cesium and rubidium). Part of the promoter is also located on the surface of Sibunit (Fig. 1).

It should be however noted that in spite of partial decoration of the active component surface accessible for the reagents (N_2 and H_2), the promoted systems exhibit much higher catalytic activity in ammonia synthesis than the non-promoted catalyst (Table 1). This fact is consistent with the suggestion that promoter chemically modifies the active component and increases the catalyst activity, thereby compensating the loss of active surface. The same conclusion about chemical modification of ruthenium under the influence of cesium compounds due to decrease in ruthenium work function has been made in our recent paper devoted to study of MgO-supported Ru catalysts [10].

Using the TEM images, size distributions of Ru particles were determined. The histograms of the particle size distributions for the promoted catalysts and non-promoted sample are compared in Fig. 3. The mean sizes of Ru particles for each samples determined using statistical analysis of the size distributions are presented in Table 2. One can see that the mean size of Ru particles in the promoted samples depends on the promoter type. Larger metal particles are observed in the Ru–Cs^+/C catalyst, whereas the use of rubidium promoter does not enlarge ruthenium particles as compared to the non-promoted sample. This result indicates that cesium is less efficient agent for preventing the agglomeration of metal particles than rubidium. Data of chemisorption measurements shown in Table 2 allow us to understand the reason of higher stability of Ru particles in the Ru–Rb^+/C samples compared with the Ru–Cs^+/C ones.

Being a maximal for the non-promoted Ru/C sample (D = 27%), accessible surface area of ruthenium decreases for the Ru–Cs^+/C sample (D = 13%), and reaches the minimal value for the Ru–Rb^+/C sample (D = 4.6%). Since the mean sizes of the Ru particles determined from TEM data are similar for the non-promoted (3.6 nm) and for the Rb-promoted (3.8 nm) samples, the observed reduction of the empty surface of ruthenium particles can be explained by a coating the ruthenium particles with a layer of promoter. Namely this coating provides the resistance of ruthenium particles against agglomeration. The reduction of the ruthenium surface accessible for CO adsorption is much less for the Cs-promoted samples and furthermore accompanied by agglomeration of the particles (TEM data). These data indicates that cesium interacts with ruthenium weaker than rubidium.

According to the X-ray diffraction data, ruthenium and cesium are in amorphous phases in all studied samples. On the other hand, the reflexes, which can be assigned to β-Rb_2O (JCPDS 27-0547) and β-Rb_2CO_3 (JCPDS 35-0973) phases (Fig. 4), were observed for the rubidium-promoted samples. Thus, the rubidium promoter occurs as a crystalline material, whereas the cesium compounds seem to be X-ray amorphous. It has been also observed that the reflexes of the support for the Ru–Cs^+/C sample are broadened as compared to other samples (Fig. 4). This suggests the disordering of the support due to interaction between Sibunit and cesium compounds.

This conclusion is supported by XPS data. As example, Fig. 5 shows original C1s core level spectra taken from pure Sibunit and from the reference Cs^+/C and Rb^+/C samples (see Sect. 2). The C1s core level binding energies (E_b) for all samples under study are listed in Table 3. The C1s spectrum of the original Sibunit is characterized by a binding energy of 284.4 eV. The promotion of Sibunit with cesium compounds followed by reduction in hydrogen shifted the C1s spectrum by 0.5 eV toward higher binding energies with respect to the initial spectrum of Sibunit (Table 3; Fig. 5). A little lower shift (0.2 eV) is observed for the Ru–Cs^+/C catalyst. Similar shifts of C1s

Table 1 Catalytic activity in NH_3 synthesis expressed as mmol(NH_3) × h^{-1} × g^{-1} (Ru) measured for different samples at 350 °C, 30 bar and 4 h^{-1}

Samples	Sequence of preparation	
	(1) metal; (2) promoter	(1) promoter; (2) metal
Ru/C	0	–
Ru–Cs^+/C	380	0
Ru–Rb^+/C	325	239

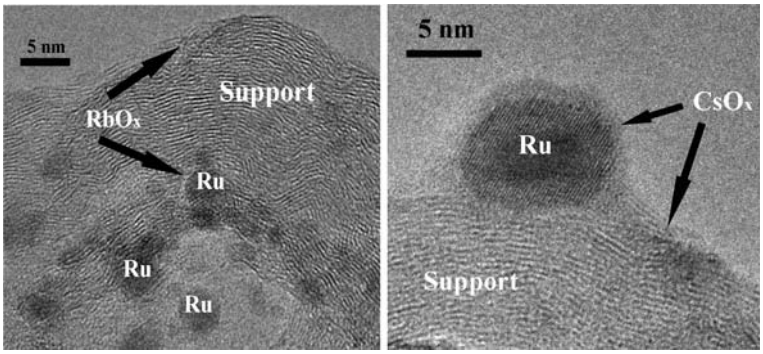

Fig. 1 TEM images for Ru–Cs^+/C (right) and Ru–Rb^+/C (left) catalysts

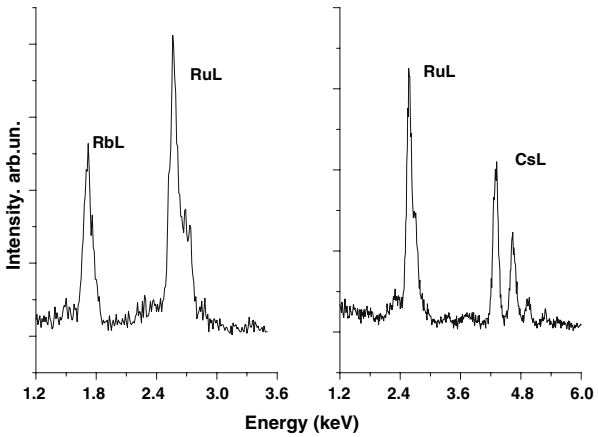

Fig. 2 EDX spectra for Ru–Cs^+/C (right) and Ru–Rb^+/C (left) catalysts

spectra to higher binding energy values were also observed for the Ru–Cs/C samples by Guraya et al. [11]. These data allows us to conclude the chemical state of carbon atoms are changed due to their interaction with cesium. This may be due to the insertion of cesium ions between carbon layers and/or the formation of intercalation compounds similar to CsC_8. Indeed, similar C1s binding energy value (285 eV) has been reported earlier by Grunes and Ritsko [12] for the intercalated compounds of graphite with alkali metals.

Such shifts are not observed for the samples promoted with rubidium compounds, which indicates the absence of substantial interaction between the rubidium promoter and the support (Table 3; Fig. 5). The formation of the bulk phase of the rubidium compounds (XRD data) is in line with the weak interaction of rubidium with Sibunit.

Analysis of the $Cs3d_{5/2}$ and $Rb3d_{5/2}$ spectra shows their shifting toward high binding energies after hydrogen treatment of the samples in the spectrometer (Fig. 6). For example, the $Cs3d_{5/2}$ spectrum of the oxidized sample promoted with cesium is characterized by E_b = 724.8 eV, whereas the reduction of the sample in the spectrometer shifts the $Cs3d_{5/2}$ to E_b = 725.3 eV. Similar shift is also observed for the Ru–Rb^+/C sample: the oxidized sample is characterized by E_b ($Rb3d_{5/2}$) = 110.5 eV, the reduced sample—by E_b ($Rb3d_{5/2}$) = 111.2 eV.

In the general case, reduction of an element decreases E_b. However, some metals (f.e. silver, cadmium, cesium, and barium) are exceptions from this rule—their binding energies is increased when the corresponding oxide transfers to metallic state [13, 14]. Not considering the reasons for these "inverse" shifts, note that in the case of cesium and rubidium, an increase in the binding energy is indicator of the reduction of promoters. As shown in our earlier works, such shifts indicate the reduction of alkali metal peroxides to suboxides [15, 16].

To confirm this assignment, the cesium-to-oxygen atomic ratios were estimated from the corresponding $Cs3d_{5/2}$ and O1s spectra. Since O1s spectra contained the signals both form cesium compounds and from the support, the difference spectra (after substitution of the spectrum from non-promoted support from the catalyst spectrum) were used for this purpose. In the oxidized sample, the Cs/O atomic ratio is close to 1.0 that suggests the formation of cesium peroxide. Reduction of the Ru–Cs^+/C sample increases this ratio to 1.8 that is in agreement with the formation of suboxide. This is an additional argument for the attribution of the $Cs3d_{5/2}$ line with E_b = 725.3 eV to cesium suboxide in the Ru–Cs^+/C sample.

In the case of the Ru–Rb^+/C catalyst, the Rb/O atomic ratio of 0.7 indicates the co-existence of rubidium peroxide (RbO_2) and superoxide (Rb_2O_2) in this sample. In the reduced Ru–Rb^+/C sample, the Rb/O atomic ratio is equal to 3.3 indicating the formation of the suboxide.

Summarizing the experimental data obtained by TEM, CO chemisorption, XPS, and XRD, we may conclude that Sibunit interacts with cesium, but its interaction with rubidium is much weaker. Then, we can explain the differences in influence of the sequence of the promoter and ruthenium introduction on catalytic properties of the Ru–Cs^+/C and Ru–Rb^+/C (see Sect. 1). The introduction of cesium before ruthenium results in strong interaction of cesium with carbon that prevents the interaction of cesium with the sequentially introduced ruthenium. As consequence, cesium does not modify ruthenium particles and

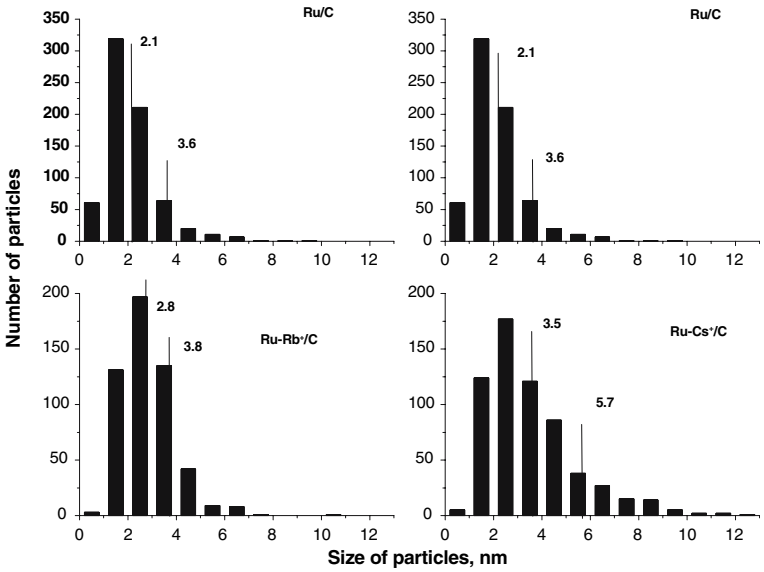

Fig. 3 Size distribution of Ru particles for Ru/C, Ru–Cs^+/C and Ru–Rb^+/C catalysts

Table 2 Ru particles sizes determined for different samples

Samples[a]	$\langle d_l \rangle$[b] (nm)	$\langle d_{vs} \rangle$[b] (nm)	D (%)[c]
Ru/C	2.1	3.6	27.0 (3.6 nm)
Ru–Cs^+/C	3.5	5.7	13.0 (7.6 nm)
Ru–Rb^+/C	2.8	3.8	4.6 (22 nm)

[a] These samples have been prepared with next sequence: ruthenium has been supported first and then—promoter

[b] $\langle d_l \rangle \Sigma n_i d_i / \Sigma n_i$, $\langle d_{vs} \rangle \Sigma n_i d_i^3 / \Sigma n_i d_i^2$

[c] Dispersion of Ru particles in different samples based on chemisorption data (and the corresponding values of particle sizes)

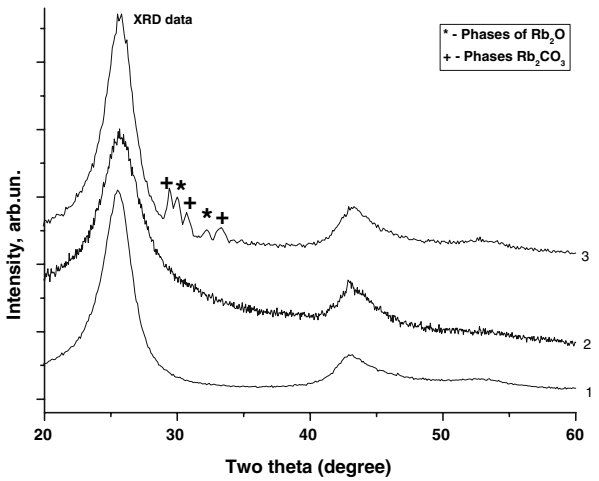

Fig. 4 XRD spectra for Sibunit (1), Ru–Cs^+/C (2) and Ru–Rb^+/C (3)

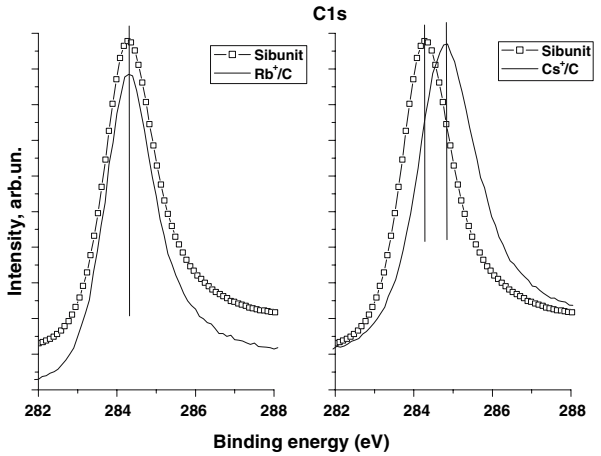

Fig. 5 C1s spectra measured for Cs^+/C and Rb^+/C samples. The spectrum from pure Sibunit is also shown for comparison

this sample does not exhibit the activity in the target reactions (similarly to the non-promoted sample). In the case of the reverse order of the cesium introduction (after formation of the ruthenium particles), cesium precursor has a possibility to interact both with the support and with ruthenium particles, which become active in ammonia synthesis. Weak interaction of the support and ruthenium results in interaction between the promoter and active component regardless of the order of their introduction.

This brings up the question: Why the cesium promoter is more effective in the interaction with Sibunit as compared

Table 3 C1s binding energies (eV) measured for different samples

Samples	Sibunit	$CsNO_3$/C	$RbNO_2$/C	Ru/C	Cs^+/C	Rb^+/C	Ru–Cs^+/C	Ru–Rb^+/C
E_{bin} (C1s)	284.4	284.4	284.4	284.4	284.9	284.4	284.6	284.4

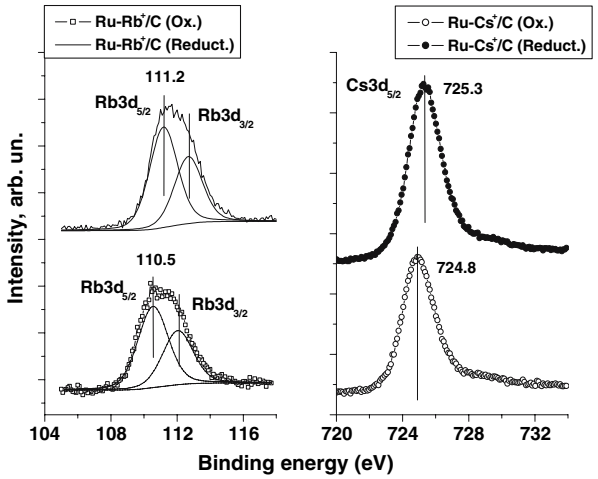

Fig. 6 $Cs3d_{5/2}$ (right) and Rb3d (left) spectra measured for Ru–Cs^+/C and Ru–Rb^+/C catalysts

to the rubidium promoter? Presumably, this phenomenon is caused by a size effect, with cesium ions or clusters being closer in size to Sibunit micropores than those of rubidium. In addition, the intercalation compound being formed seems to be more stable with cesium rather than with rubidium.

4 Conclusions

(1) The use of cesium as a promoter results in its strong interaction with the support (Sibunit). The promoter occurs both as cesium ions inserted into the support micropores and as a free cesium suboxide ($Cs_{2+x}O$). In the presence of ruthenium, the competitive metal–promoter and support–promoter interactions proceed in the system, which leads to a significant redistribution of the promoter and variation in the catalyst activity depending on the sequence of operations during its preparation.

(2) If the catalyst is promoted with rubidium, the interaction between the promoter and support is not observed. Thus, here the catalytic properties depend only slightly on the order of catalyst preparation.

(3) In the oxidized samples promoters are in the form of peroxide with some admixture of oxide in the case of the rubidium-promoted samples. The promoters can be reduced to suboxide due to the metal–promoter interaction (ruthenium serves as an activator of hydrogen).

Acknowledgments The authors are grateful to N. M. Dobrynkin, V. I. Zaikovskii, L. B. Okhlopkova and A. S. Lisitsyn for their assistance in testing the samples.

References

1. Nielsen A, Topsøe H (1995) Ammonia. Catalysis and manufacture. Springer-Verlag, New York
2. Schlögl R (1997) In: Ertl G, Knozinger H, Weitkamp J (eds) Handbook of heterogeneous catalysis, vol 4. Wiley-VCH, Weinheim
3. Rarog W, Kowalczyk Z, Sentek J, Skladanowski D, Zielinski J (2000) Catal Lett 68:163
4. Kowalczyk Z, Jodzis S, Rarog W, Zielinski J, Pielaszek J (1998) Appl Catal A 173:153
5. Aika K, Ohya A, Ozaki A, Inoue Y, Yasumori I (1985) J Catal 92:305
6. Shitova NB, Dobrynkin NM, Noskov AS, Prosvirin IP, Bukhtiyarov VI, Kochubey DI, Tsyrul'nikov PG, Shlyapin DA (2004) Kinet Catal 45:414
7. Ermakov YuI, Surovikin VF, Plaksin GV, Semikolenov VA, Likholobov VA, Chuvilin AL, Bogdanov SV (1987) React Kinet Catal Lett 32:435
8. Moulder JF, Stickle WF, Sobol PE, Bomben KD (1992) Handbook of X-ray photoelectron spectroscopy. Perkin-Elmer Corporation
9. Muhler M, Rosowski F, Hinrichsen O, Hornung A, Ertl G (1996) In: Hightower JW, Delgass WN, Iglesia E, Bell AT (eds) Studies in Surface Science and Catalysis, vol 101. Elsevier, Berlin, p 317
10. Larichev YV, Moroz BL, Zaikovskii VI, Yunusov SM, Kalyuzhnaya ES, Shur VB, Bukhtiyarov VI (2007) J Phys Chem C (in press, published on Web at 06/05/2007)
11. Guraya M, Sprenger S, Rarog-Pilecka W, Szmigiel D, Kowalczyk Z, Muhler M (2004) Appl Surf Sci 238:77
12. Grunes LA, Ritsko JJ (1983) Phys Rev B 28:3439
13. Ebbinghaus G, Simon A (1997) Chem Phys 43:117
14. Hwang CC, An KS, Park RJ, Kim JS, Lee JB, Park CY, Lee SB, Kimura A, Kakizaki A (1998) J Electron Spectrosc Relat Phenom 88:733
15. Podgornov EA, Prosvirin IP, Bukhtiyarov VI (2000) J Mol Catal A 158:337
16. Larichev YV, Prosvirin IP, Shlyapin DA, Shitova NB, Tsyrul'nikov PG, Bukhtiyarov VI (2005) Kinet Catal 46:597